FUTURE RAINFALL CHARACTERISTICS UNDER AR6 CLIMATE CHANGE SCENARIOS, CASE STUDY OF PASAK RIVER BASIN, THAILAND

Ketvara Sittichok
Kasetsart University, Thailand
fengkrs@ku.ac.th

Abstract Thailand is located in Southeast Asia where it is indicated as highly vulnerable to climate change. This country will likely be one of the countries that have experienced negative impacts of climate change. To reduce the impact of climate change on drought and flood, a water management plan under climate change needs to be prepared. The changes of future rainfalls under climate change emission scenarios play an important role and need to be investigated. This study aims to describe projected rainfall characteristics under AR6 climate change scenarios. Rainfalls generated from 10 GCMs were downscaled to a basin scale at the Pasak River Basin using the quantile mapping method. After the downscaling process simulated precipitation significantly improved in both magnitude and volume compared to the observed data using the Nash-Sutcliff coefficient and volume error methods. Slight differences between downscaled and observed precipitation were found with acceptable results using the coefficient of determination. Variabilities of future precipitation under four scenarios (SSP1-2.6, SSP2-4.5, SSP3-7.0 and SSP5-8.5) of each model were revealed. Annual average of projected rainfalls was slightly different between the models, but large variation compared to others could be found in INM-CM5. The standardized anomaly index was then calculated for historical and two future periods: the near-term (2015-2050) and the long-term (2051-2100), and the frequencies of wet and dry incidents were presented. Very-extremely wet and dry years often occurred in 2051-2100 under SSP2-4.5 and SSP1-2.6 respectively. Finally, the increments in annual rainfalls were obviously seen in SSP2-4.5, SSP3-7.0 and SSP5-8.5 for the near-term and in all scenarios of the long-term. Slight decreasing trend was only found in the near-term under SSP1-2.6.

Keywords: AR6 emission scenarios, climate change, quantile mapping method, standardized anomaly index.

Introduction

There have been evidences of the impacts of climate change on precipitations in various regions of the globe. Global warming leads to the changes of extreme precipitation and flood intensities at the end of the 21 century in different climate regions [1; 2]. In addition, a mean global sea level also rises and other extreme events such as typhoons and droughts increase. Thailand is located in Southeast Asia where it is indicated as highly vulnerable to climate change [3; 4]. This country will likely be one of the countries that have experienced negative impacts of climate change due to its geography, socio-economic issues and level development [5]. Livelihood of people in the country mainly relies on agriculture, and therefore meteorological changes, especially precipitation and temperature, are conductive to the growth of agricultural products. As evidenced the recent droughts and floods related to climate change resulted in numerous disasters in the country. Thailand faced severe flooding in 2011, and the worst droughts in decades occurred in 2015-2016 [6]. The adverse impacts of climate change take place not only in the country but also the conflict between Thailand and its neighbours could be plausibly found especially in water management [5].

New nine Shared Socioeconomic Pathways (SSPs) have been launched according to a new phase of model experiment the Sixth Assessment Report (AR6) prepared by the Intergovernmental Panel on Climate Change (IPCC). There are five high priority scenarios with four groups of SSP indicated in Tier 1 (SSP1, SSP2, SSP3 and SSP5). Two emission scenarios (SSP1-1.9 and SSP1-2.6) in SSP1 present a low challenge group. SSP1-1.9 reflects 1.5 ºC that is a target of the Paris Agreement. SSP1-2.6 corresponds to RCP 2.6 indicated in the previous scenario of the Fifth Assessment Report (AR5). SSP2-4.5 presents the scenario in the middle of the road which reflects the RCP 4.5 under the AR5 experiment. SSP3-7.0 and SSP5-8.5 scenarios fall in a category of medium-high range and the highest level of AR6, respectively. SSP3-7.0 is in the regional rivalry of socio-economic family and SSP5-8.5 indicates the highest use of fossil of the 21st century [7].

In the complicated climate system, climate factor changes can be investigated using General Circulation Models (GCMs) which play an important role for the climate change research area. Over 50 GCMs with more than 20 institutions collaborate on the Coupled Model Intercomparison Project (CMIP6). GCMs are capable to develop projections of main climate factors under various greenhouse gas emission scenarios with consideration of the socio-economic status. The differences between the models can be found mostly due to the model calculations, climate system variability and the implication

of socio-economic factors applied in the models. Even though, the projections generated using GCMs usually agree in the overview, the results of specific local area should be more concerned due to low spatial resolution of most GCMs [8]. This leads to a downscaling process needed to be initially applied with the GCMs' outputs [9, 10].

To gain the knowledge of rainfall characteristics under AR6 climate change scenarios in a basin scale at the Pasak River basin, rainfall projections of four scenarios in Tier 1 (SSP1-2.6, SSP2-4.5. SSP3-7.0, SSP5-8.5) simulated from 10 GCMs were investigated in this study. Only GCMs generated under all four scenarios with 100 km spatial resolution were considered. All rainfall simulations were initially downscaled using the quantile mapping method. Observed rainfalls at eight stations in and around the basin were compared to downscaled rainfalls during the historical period. Three statistical measures that were the coefficient of determination, Nash-Sutcliff coefficient and the volume error methods were employed in this study. Standardize anomaly index values of future rainfalls were then calculated to examine the frequency of wet/dry incidents during both historical and future periods under all climate change scenarios. The trends of projected precipitation of all scenarios were also explored. The results of this research will be continuously applied together with a rainfall-runoff model to estimate water balance and flood/drought risks in the basin in the near future. This will benefit for the water management policy and adaptation plan for this area.

Materials and methods

1) Study area

The Pasak River basin is one of 22 main basins in Thailand located in the central part of the country with the area of 15,562 km2. Pasak River is the main channel of the basin with the length of 700 km. This basin covers seven provinces comprising of eight sub-basins (Figure 1). The Pasak Jolasid dam is the main dam with the capacity storage of the reservoir around 960 mcm. The rainy season of the basin is in between August and October. The main land use of this area is forest followed by rice crop and field crops. The basin has experienced both floods and droughts due to rainfall variation, the physical topography and natural deterioration.

2) Data collection

(1) Precipitation of GCMs

Historical (1980-2014) and projected precipitation of four scenarios which were SSP1-2.6, SSP2-4.5, SSP3-7.0 and SSP5-8.5 (2015-2100) in Tier1 developed by 10 GCMs were collected. Only GCMs generated results with 100 km at daily time step and under all four scenarios indicated above were selected. All selected GCMs are the Atmospheric-Ocean General Circulation Models (AOGCMs) comprising of biogeochemical function, for example, vegetation and some atmospheric chemistry in the model (11). This study paid attention to only variant label of r1i1p1f1 where r, i, p and f refer to the realization index, initialization index, physical index and the forcing index, respectively. Table 1 presents the list of selected models.

(2) Observed precipitation

Observed precipitations during 1985-2016 were collected from eight climate stations located inside and around the basin prepared by the Thai Meteorological Department (Figure 1). Annual precipitations of all stations were between 1,007 and 1,265 mm/year. Thiessen method was applied to calculate aerial average precipitation showing annual precipitation of the basin around 1,141 mm/year. The maximum rainfall usually occurs in September.

3) Quantile mapping method

Precipitation data generated using selected GCMs were downscaled using the quantile mapping bias correction widely used for precipitation downscaling [12; 13]. This statistical method is non-parametric bias correction which is strongly advantageous to be applied for most possible distributions. Their adjustment can be described in terms of their empirical cumulative distribution function and its inverse presenting in Equation 1. The empirical cumulative distribution function (*ecdf*) and its inverse ($ecdf^{-1}$) were applied in the method. P_{sim} refers to the simulated precipitation on the t^{th}. $ecdf_{sim}$ and $ecdf_{obs}^{-1}$ represents the empirical cumulative distribution function of simulations and its inverse of the observed data, respectively. Finally, corrected precipitation was calculated.

In this study, historical simulations of all GCMs were tested using the quantile mapping method with the observed data of each station during 1985-2014. New precipitation data in this period were then compared to observations and three statistical measures were then reported. Future period of all GCMs and all scenarios (2015-2100) with empirical cumulative distribution of the observe data of each station were then calculated in the process of bias correction.

$$P_{cor(t)} = ecdf_{obs}^{-1}\left(ecdf_{sim}\left(P_{sim}(t)\right)\right). \quad (1)$$

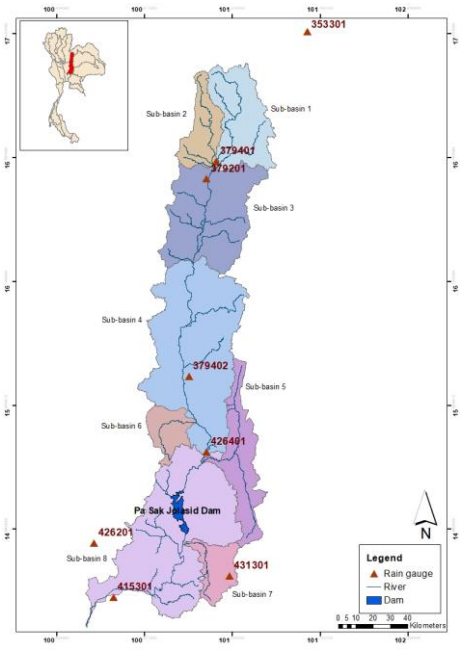

Fig. 1. **Study area and location of climate stations**

Table 1

GCMs used in this study

GCM	Institution	GCM	Institution	GCM	Institution
CESM2-WACCM	National Center for Atmospheric Research	GFDL-ESM4	Geophysical Fluid Dynamics Laboratory, USA	MPI-ESM1-2-HR	The Max Planck Institute for Meteorology, Germany
CMCC-CM2-SR5	Euro-Mediterranean Centre on Climate Change Coupled Climate Model	INM-CM4-8	The Institute for Numerical Mathematics, Russia	MRI-ESM2-0	The Meteorological Research Institute, Japan
CMCC-ESM2	Euro-Mediterranean Centre on Climate Change Coupled Climate Model	INM-CM5-0	The Institute for Numerical Mathematics, Russia	NorESM2-MM	Norwegian Earth System Model
				TaiESM1	Taiwan Earth System Model

4) Standardized anomaly index (SAI)

Standardized anomaly index (SAI) is usually applied to investigate precipitation conditions in various areas [14-16]. It is cable to explain rainfall variability and also to determine the frequency of dry and wet incidents. Annual rainfall of each year is calculated and the deviations from the average annual rainfall in the study period were computed. Negative\positive SAI values reflecting lower/higher rainfall compared to the average rainfall that is risky to drought\flood event are finally calculated. Equation 2 presents the method to compute SAI. Xi is the annual rainfall of year *i*, and μ and δ is the average and standard deviation of long-term rainfall period, respectively. SAI values can be classified

into 7 groups with three main categories: dry (-1.0 to > -2.0), wet (1.0 to > 2.0) and normal (-0.99 to 0.99) indicated in Table 2.

$$SAI_i = \frac{X_i - \mu}{\delta}. \quad (2)$$

Table 2

SAI classification

Dry incident		Near normal	Wet incident	
SAI	**Category**	**SAI**	**SAI**	**Category**
-2.0 and less	Extremely dry	-0.99 to 0.99	2.0 +	Extremely wet
-1.5 to -1.99	Severely dry		1.5 to 1.9	Very wet
-1.0 to -1.49	Moderate dry		1.0 to 1.49	Moderate wet

Results and discussion

1) Precipitation downscaling estimation

Simulated precipitations during the historical period (1985-2014) of all ten models were downscaled to climate stations using the quantile mapping method. Three statistical measures that were the correlation coefficient (R), Nash-Sutcliff coefficient (NSE) and percentage of volume error (VE) generally applied to estimate downscaling results were employed in this study [17; 18]. The ranges of R and NSE are -1 to 1 and -∞ to 1 respectively, while VE are in between 0 to ∞. Equation 3-5 presents the formulas of all three measures when obs and sim was observed and simulated data of month i for all n months. Original precipitation of GCMs and downscaled precipitation were compared to observed precipitation (GCM-Obs/Qmap-Obs) for each climate station. The results revealed that original precipitation of all models for most stations generally produced R in between 0.7-0.8 compared to the observed data and there was no significant difference of R between GCM-Obs and Qmap-Obs. However, large differences in terms of magnitude and volume of precipitation between GCM-Obs and Qmap-Obs could be obviously seen for all stations and models. Negative or zero values of NSE of GCM-Obs were strongly improved to positive values after the downscaling process presenting in most models especially in CMCC-CM2 (NSE of GCM-Obs: -0.4 to 0.0/NSE of Qmap-Obs: 0.3-0.5). VE values were also significantly decreased for all models. Large differences before and after the downscaling process were clearly seen, especially in INM-CM4, INM-CM5 and GFDL. Table 3 presents details of NSE and VE of both GCM-Obs and Qmap-Obs for all stations and all models.

$$R = \frac{\sum_{i=1}^{n}\left(obs_i - \overline{obs}\right)\left(sim_i - \overline{sim}\right)}{\sqrt{\sum_{i=1}^{n}\left(obs_i - \overline{obs}\right)^2 \sum_{i=1}^{n}\left(sim_i - \overline{sim}\right)^2}}, \quad (3)$$

$$NSE = 1 - \frac{\sum_{i=1}^{n}\left(obs_i - sim_i\right)^2}{\sum_{i=1}^{n}\left(obs_i - \overline{obs}\right)^2}, \quad (4)$$

$$VE = \frac{\left|sim_i - obs_i\right|}{obs_i} * 100. \quad (5)$$

2) Precipitation projections of Pasak River Basin

(1) The differences of projected precipitation between GCMs

The projected precipitations under all four scenarios generated using each GCM and downscaled using the quantile mapping method were investigated. Figure 2 presents statistical characteristics of all annual precipitations during the period of 2015-2100. Average precipitation of the basin was calculated using the Thiessen method. Average annual precipitations during 2015-2100 of all scenarios for all models were slightly different with the range of 1,071-1,100 mm. Maximum rainfalls for SSP1-2.6 and SSP2-4.5 could be found in MRI-ESM2 rising up to 1,696 and 1,631 mm, respectively. SSP3-7.0 and

SSP5-8.5 scenarios showed the highest annual rainfall of 1,777 and 1,742 mm with INM-CM5 and CMCC-ESM2, respectively. Large variability of projected data could be obviously seen in INM-CM5 under three scenarios (SSP1-2.6, SSP3-7.0 and SSP5-8.5) compared to other models. INM-CM4 and INM-CM5 mostly presented the lowest precipitation for all scenarios, except SSP3-7.0. Positive outliers of the rainfall data for SSP1-2.6 and SSP2-4.5 occurred with MRI-ESM2 and CMCC-ESM2, while TaiESM1 also gave outlier under SSP3-7.0.

Table 3

Nash-Sutcliff coefficient and volume error of GCM-Obs and Qmap-Obs

Model		Station							
		353301	**379401**	**379201**	**379402**	**426401**	**426201**	**431301**	**415301**
CESM2	*NSE /VE	0.2/15	0.2/17	0.1/20	0.3/18	0.3/17	0.3/16	0.3/17	0.3/16
	NSE/ VE	-1.6/60	-1.8/70	-1.8/70	-1.5/62	-1.5/62	-1.2/54	-1.8/68	-1.3/58
CMCC_ CM2	*NSE /VE	0.5/15	0.4/16	0.3/16	0.5/14	0.5/14	0.5/15	0.5/15	0.5/17
	NSE/ VE	0.1/33	-0.1/40	0.0/40	0.0/39	0.0/40	-0.4/58	-0.1/52	0.0/43
CMCC_ ESM2	*NSE /VE	0.4/18	0.3/22	0.2/25	0.3/20	0.3/18	0.3/19	0.4/17	0.4/16
	NSE/ VE	0.0/32	0.0/36	0.0/37	0.0/34	0.0/33	-0.3/47	0.0/41	0.2/33
GFDL	*NSE /VE	0.2/15	0.0/16	0.0/18	0.1/16	0.0/15	0.3/14	0.2/15	0.2/14
	NSE/ VE	-1.1/35	-2.5/63	-2.4/62	-2.2/57	-2.2/58	-2.2/59	-2.0/54	-1.6/50
INM-CM4	*NSE /VE	-0.2/20	-0.3/22	-0.4/22	0.1/19	0.1/20	0.3/15	0.0/17	0.2/16
	NSE/ VE	-4.4/H	-4.6/H	-4.4/H	-1.3/H	-1.4/H	-2.0/H	-1.1/H	-1.4/H
INM-CM5	*NSE /VE	0.0/15	-0.2/16	-0.2/17	0.0/23	0.0/23	0.2/22	0.1/24	0.2/23
	NSE/ VE	-6.6/H	-6.8/H	-6.5/H	-3.0/H	-3.0/H	-2.5/H	-1.4/H	-1.8/H
MPI-ESM1	*NSE /VE	0.2/16	0.0/18	0.0/21	0.2/16	0.2/15	-0.1/20	0.1/16	-0.2/18
	NSE/ VE	0.2/16	-0.1/18	0.0/21	-0.1/20	-0.1/19	-1.9/56	-0.6/27	-1.4/48
MRI-ESM2	*NSE /VE	0.0/20	0.0/22	0.0/24	0.0/19	0.0/19	0.1/18	0.1/17	0.1/16
	NSE/ VE	-0.5/27	-0.6/30	-0.5/31	-0.6/31	-0.7/30	-0.5/24	-0.6/26	-0.6/23
NorESM 2	*NSE /VE	0.2/22	0.2/24	0.1/26	0.3/21	0.3/20	0.3/22	0.4/20	0.4/20
	NSE/ VE	-1.2/54	-1.0/56	-1.0/56	-0.5/46	-0.5/46	-0.6/33	-0.6/48	-0.3/42
TaiESM 1	*NSE /VE	0.3/16	0.3/15	0.3/16	0.4/15	0.4/15	0.4/14	0.4/15	0.4/15
	NSE/ VE	0.2/21	0.1/32	0.1/32	0.1/31	0.1/30	-0.5/51	0.0/39	0.1/32

Remark: *: Qmap-Obs /non: GCM-Obs/H: higher than 100%

(2) Standardized anomaly index of precipitations

To estimate rainfall characteristics under different scenarios of the basin, daily projected rainfalls of all models for each SSP scenario were averaged. SAI values of two periods: the near-term (2015-2050) and the long-term (2051-2100) were then computed and compared to the SAI values of the observed data. As mentioned above, SAI is categorized into seven categories with positive/negative values referring to wet/dry years respectively. SAI values of each SSP and the observed rainfall data which were in moderate to extremely wet/dry categories are presented in Figure 3. Very-extremely wet never occurred in the historical period, while the basin faced extremely dry incident in 2001. During the near-term, SSP5-8.5 gave projected precipitation with the highest SAI of 2.75 showing extremely wet

in 2035. Very wet to extremely wet (SAI of 1.5 to higher than 2.0) occurred in 13 years with 4 years under SSP2-4.5, 4 years under SSP 3-7.0, 3 years under SSP1-2.6, and 2 years under SSP5-8.5. Extremely dry in this period occurred in 2016 and 2049 under SSP4-8.5 and SSP1-2.6, respectively. Severely to extremely dry incidents were presented in 10 years with 4 years of SSP5-8.5, 3 years of SSP1-2.6, 2 years and only 1 year of SSP2-4.5 and SSP3-7.0, respectively.

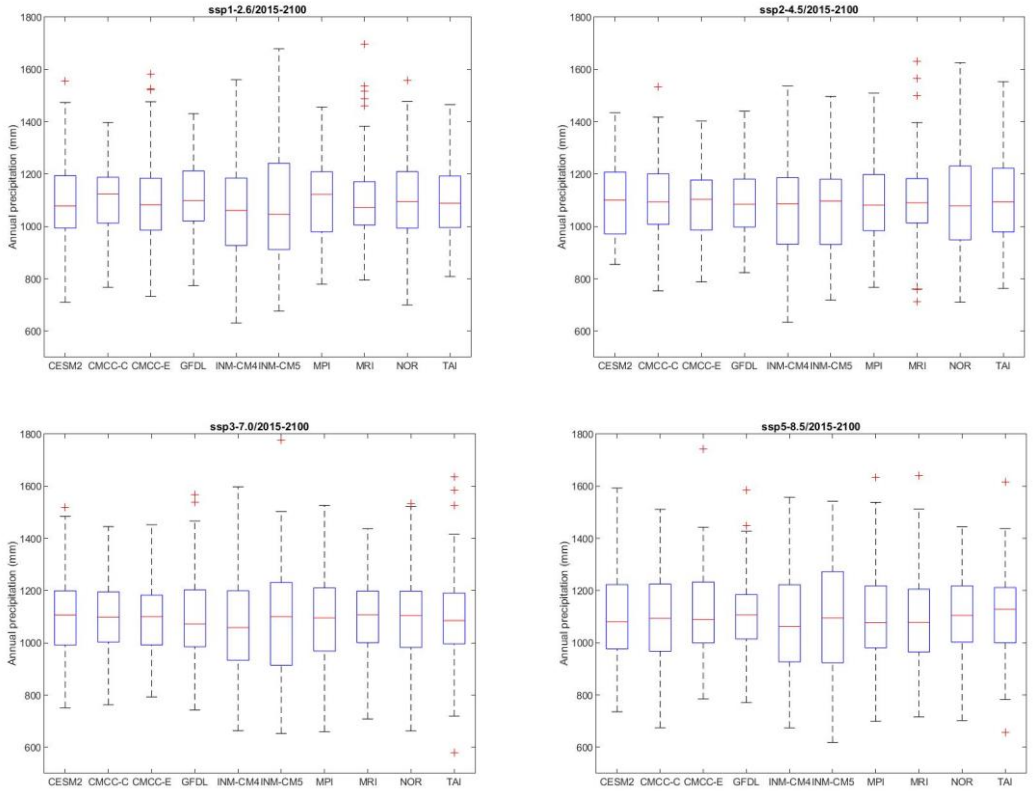

Fig. 2. **Comparison of projected precipitations of 10 GCMs under four scenarios**

Both extremely wet and dry occurrences largely occurred in the long-term compared to the near-term. There were 7 years of this period showing extremely wet under different scenarios with the highest one occurring in 2096 under SSP2-4.5 (SAI of 3.0). SAI values of 15 years were in very – extremely wet class. Rainfall projection of SSP2-4.5 presented the highest frequent of very – extremely wet occurrence (6 years), followed by SSP5-8.5 simulations (5 years). Severely to extremely dry incidents also occurred more often with the lowest SAI in 2051 of SSP3-7.0. There were 14 years out of 50 years presented severely to extremely dry with the most frequent showed under the simulations of SSP1-2.6 (7 years) followed by SSP2-4.5 (3 years).

It was noticeably seen that there were the same events occurring in some years with different SSP scenarios, especially in the long-term period. There were three incidents of moderate to extremely dry in 2051 (SSP3-7.0/SSP1-2.6/SSP5-8.5) and 2067 (SSP3-7.0/SSP1-2.6/SSP2-4.5). It is also worth to mention that contradict results of different SSP scenarios are obviously seen in both periods; for example, in 2035, 2040, 2046, 2085 and 2091.

(3) Trends of precipitation

Annual projected precipitation time series are presented in Figure 4. In the near-term, average annual rainfalls between 2015 and 2050 of four SSPs were insignificantly different with the range of 1,062 – 1,082 mm and standard deviations were in between 48 and 56 mm. Simulation of SSP1-2.6 presented slightly rainfall decrease which was absolutely different from other SSPs. The increase of rainfalls highly occurred in SSP2-4.5 and SSP5-8.5 while slightly increment was also found in SSP3-7.0. Both annual maximum and minimum projected rainfalls were generated under SSP5-8.5 in 2035 (1,210 mm) and 2016 938 mm), respectively. This result was correspondent to SAI results mentioned in the previous section.

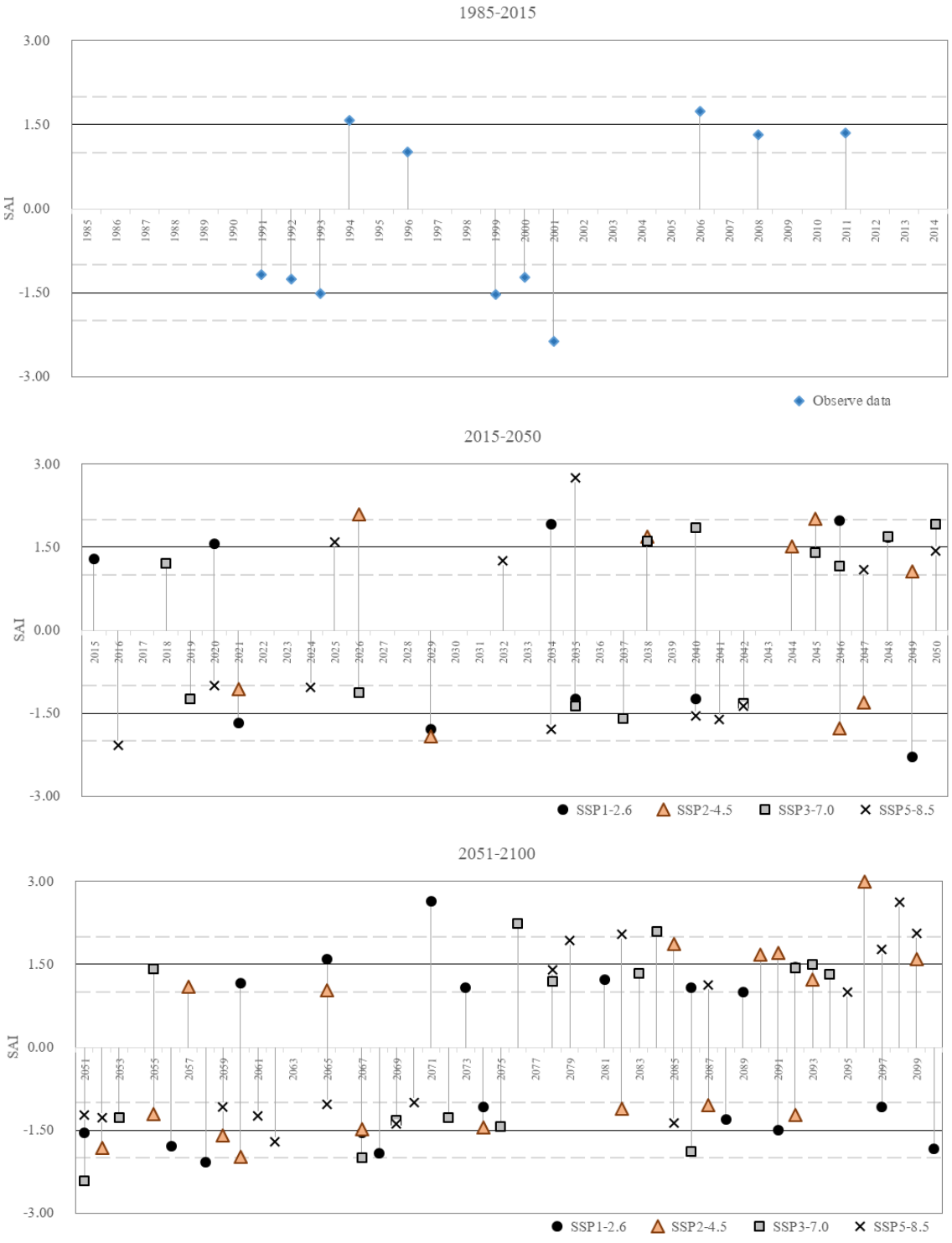

Fig. 3. **SAI of historical and projected precipitation under each SSP scenario**

In the long-term, average annual precipitations and standard deviation were in the range of 1.105-1.124 mm and 46-66 mm, respectively. The largest increments of projected rainfalls exhibited in SSP5-8.5. SSP2-4.5 and SSP3-7.0 also showed significant rainfall increase similar to the near-term. Insignificant increase was found in SSP1-2.6. Maximum rainfalls were projected under SSP2-4.5 and SSP5-8.5 (1,296 mm) corresponding to wet incidents indicated in the previous section. The lowest annual rainfall occurred in 2051 with SSP 3-7.0.

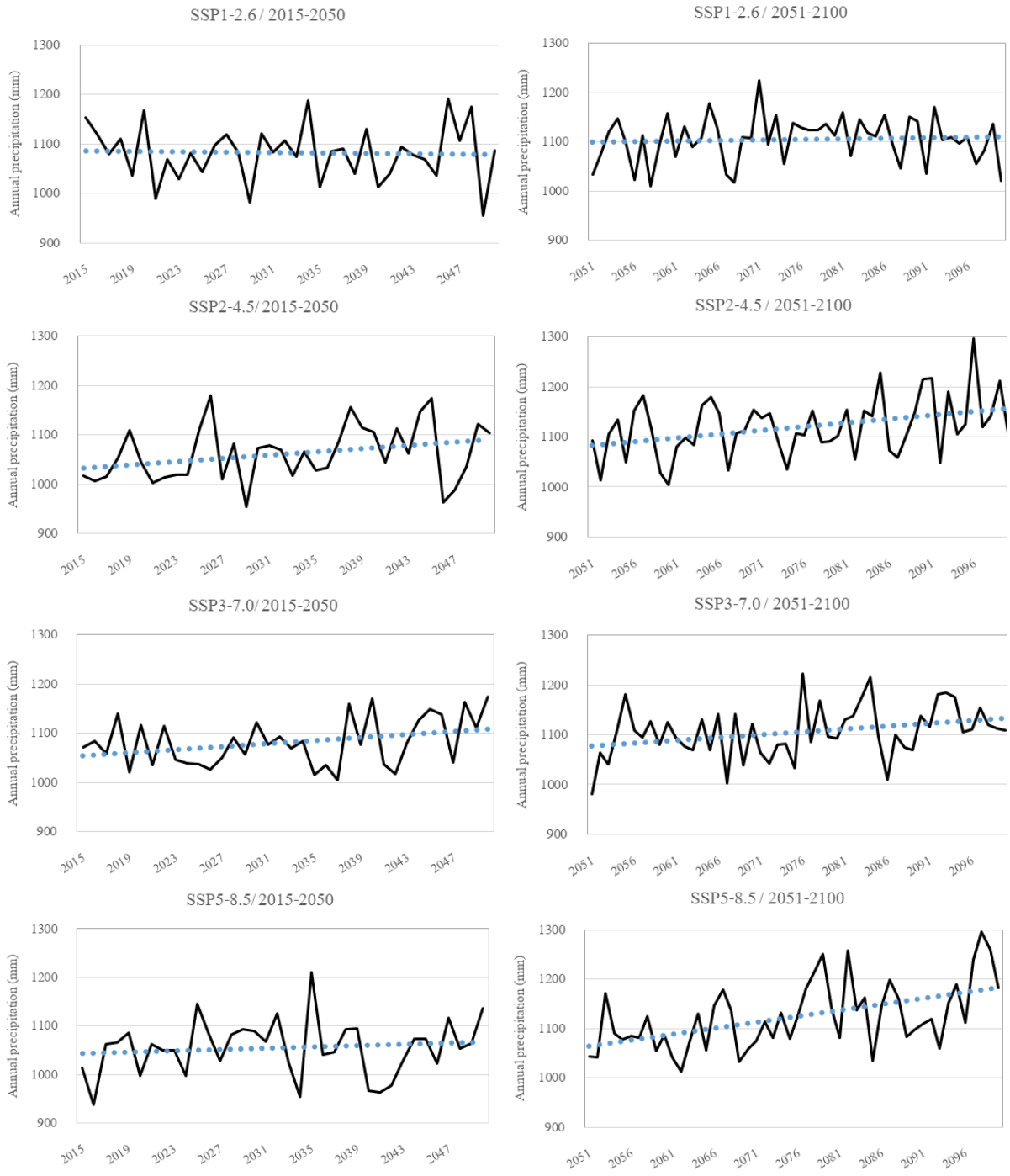

Fig. 4. **Annual projected precipitation trends of four scenarios**

Conclusion

This study generated plausible future precipitation for the Pasak River Basin, Thailand under four scenarios (SSP1-2.6, SSP2-4.5, SSP3-7.0 and SSP5-8.5) of AR6 which have been launched. Characteristics of precipitation projections developed by 10 GCMs at the basin scale were described. Only GCMs generated results with 100 km resolution for the four scenarios were selected in this study. The quantile mapping method was initially applied to downscale GCMs' precipitations to a basin scale for eight climate stations. Downscaled rainfalls of the historical period (1985-2014) were compared to the observe data and explained with the three statistic measures: coefficient of determination (R), Nash-Sutcliffe coefficient (NSE) and volume error (VE).

The results revealed that NSE and VE significantly improved after the downscaling process and small changes in R were found with acceptable results with R in between 0.7-0.8 and the highest NSE of 0.5. Projected rainfall characteristics for the entire period of 2015-2100 of each GCMs and each emission scenario for the basin were then presented. Large variability of the data could be obviously seen in INM-CM5 for three scenarios. Outliers in projected precipitation were remarkably detected in MRI-ESM2 for SSP1-2.6 and SSP2-4.5 and in TaiESM1 for SSP3-7.0.

SAI was then computed to estimate wet - dry incidents for the historical (1985-2014) and future periods: the near-term (2015-2050) and the long-term (2051-2100). No extremely wet and only one incident of extremely dry occurred in the basin during 1985-2014. Very to extremely dry and wet occurred more often in the long-term compared to the near-term. Very to extremely wet years of both future periods often occurred under SSP2-4.5 and SSP3-7.0 respectively, while severely to extremely dry mostly happened under SSP1-2.6/SSP5-8.5. Finally, the trends of rainfall projections were showed. Increase in precipitation under SSP5-8.5 of the long-term was significantly higher than other scenarios which climbed up to 1,296 mm. Precipitations of SSP2-4.5 and SSP3-7.0 for both periods were also rising. Decreasing trends could be found only under SSP1-2.6 with the near-term. Climate change scenarios of CMIP6 were also studied in various regions; for example, duration of rainy season was found to be extended for the monsoon domains over India, Indochina peninsula, and Southern Africa under SSP5-8.5 for the long-term period [19]. The increasing trend of rainfall during wet season also was indicated in Malaysia and the long-term period showed significantly higher compared to the near-term [20].

For the future work, all results of this research will be continued to apply for the flood and drought risk management plan. Rainfall projection of each station and each scenario will be analysed to seek for plausible extreme events affecting livelihood in the area. Hydrological models will get involved in the near future to simulate extreme drought and flood incidents at specific locations in the basin. Risk maps of both flood and drought under climate change in this area will be published together with practical adaptation plans.

References

[1] Tabari H. Climate change impact on flood and extreme precipitation increases with water availability. Scientific Report, vol.10, 2020. 13768 p.
[2] Kirchmeier-Young M.C. and Zhang X. Human influence has intensified extreme precipitation in North America. PNAS, vol.117, 2020, pp. 13308-13313.
[3] ADB. The Economics of Climate Change in Southeast Asia: A Regional Review, ISBN 978-971-561-787-1, 2009.
[4] Hijioka Y., Lin E., Pereira J.J., Corlette R.T., Cui X., Insarov G.E., Lasco R.D., Lindgren E., Surjan A. Asia in: Climate Change: Impacts, Adaptation, and Vulnerability. Part B: Regional Aspects, Contribution of Working Group II to the Fifth Assessment Report of Intergovernment Panel on Climate Change, 2014.
[5] Marks D. Climate change and Thailand: impact and response. Contemporary Southeast Asia, vol. 33, 2011, pp. 229-258.
[6] Naruchaikusol S. Climate change and its impact in Thailand. TransRe Fact Sheet, vol.2, 2016, pp.1-16.
[7] Meinshausen M., etc. The shared socio-economic pathway (SSP) greenhouse gas concentrations and their extension to 2500. Geoscientific Model Development, vol.13, 2020, pp. 3571-3605.
[8] Raty O., Raisanen J., Ylhaisi J. Evaluation of delta change and bias correction methods for future daily precipitation: intermodal cross-validation using ENSEMBLES simulations. Climate Dynamics: observational, theoretical and computational research on the climate system, vol. 42, 2014, pp. 2287-2303.
[9] Jacobeit J., Hertig E., Seubert S., Lutz K. Statistical downscaling for climate change projections in the Mediterranean region: methods and results. Regional Environmental Change, vol. 14, 2014, pp. 1891-1906.

[10] Liu J., Yuan D., Zhang L., Zou X., Song X. Comparison of three statistical downscaling methods and ensemble downscaling method based on Bayesian model averaging in upper Hanjiang River Basin. Advances Meteorology, 2015, 7463963 p.
[11] Flato G., Marotzke J., Abiodun B., Braconnot P., Chou S.C., Collins W., Cox P., Driouech F., Emori S., Eyring V., Forest C., Gleckler P., Guilyardi E., Jakob C., Kattsov V., Reason C. and Rummukainen M. Evaluation of Climate Models. In: Climate Change 2013, IPCC, 2013.
[12] Bertrand D., McPherson R.A. Development of downscale climate projections: a case study of the Red River Basin, South-Central U.S. Advances in Meteorology, vol. 2019, 2019, 4702139 p.
[13] Miao Q., Pan B., Wang H., Hsu K., Sorooshian S. Improving monsoon precipitation prediction using combined convolutional and long short term memory neural network. Water, vol. 11, 2019, 977 p.
[14] Eshetu G., Johansson T., Garedew W. Rainfall trend and variability analysis in Setema-Gatira area of Jimma, Southwestern Ethiopia, African Journal of Agricultural Research. vol. 11, 2016, pp. 3037-3045.
[15] Koudahe K., Kayode A.J., Samson A.O., Adebola A.A., Djaman K. Trend analysis in standardized precipitation index and standardized anomaly index in the context of climate change in Southern Togo. Atmospheric and Climate Sciences, vol. **7,** 2017, pp. 401-423.
[16] Bayable G., Amare G., Alemu, G., Gashaw T. Spatiotemporal variability and trends of rainfall and its association with Pacific Ocean seas surface temperature in West Harerge zone, Eastern Ethiopia. Environmental System Research. vol. 10, 2021, pp. 1-21.
[17] Anuchaivong P., Sukawat D., Luadsong A. Statistical downscaling for rainfall forecasts using modified constructed analog method in Thailand. The Scientific World Journal, vol. 2017, 2017. 1075868 p.
[18] Birara H., Pandey R.P., Mishra S.K. Projections of future rainfall and temperature using statistical downscaling techniques in Tana Basin. Sustainable Water Resources Management, vol. 6, 2020.
[19] Moon S., Ha K.J. Future changes in monsoon duration and precipitation using CMIP6. Climate and Atmospheric Science, vol. 3, 2020, pp. 1-7.
[20] Adib M.N., Harun S., Rowshon, K. Long-term rainfall projection based on CMIP6 scenarios for Kurau River Basin of rice-growing irrigation scheme, Malaysia. SN Applied Sciences, vol. 4, 2022, pp. 1-14.